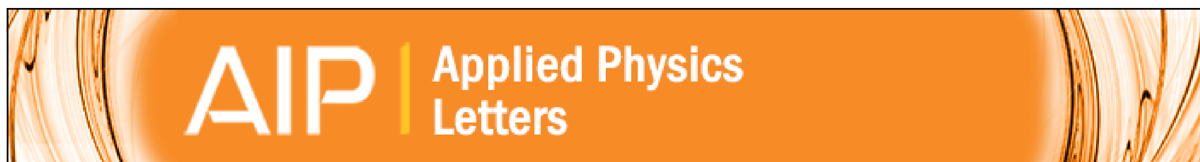

Cavity-enhanced resonant tunneling photodetector at telecommunication wavelengths

Andreas Pfenning, Fabian Hartmann, Fabian Langer, Sven Höfling, Martin Kamp, and Lukas Worschech

Citation: Applied Physics Letters **104**, 101109 (2014); doi: 10.1063/1.4868429
View online: http://dx.doi.org/10.1063/1.4868429
View Table of Contents: http://scitation.aip.org/content/aip/journal/apl/104/10?ver=pdfcov
Published by the AIP Publishing

Articles you may be interested in
GaAs/AlGaAs resonant tunneling diodes with a GaInNAs absorption layer for telecommunication light sensing
Appl. Phys. Lett. **100**, 172113 (2012); 10.1063/1.4709421

Quantum dot resonant tunneling diode for telecommunication wavelength single photon detection
Appl. Phys. Lett. **91**, 073516 (2007); 10.1063/1.2768884

Demonstration of low-cost Si-based tunable long-wavelength resonant-cavity-enhanced photodetectors
Appl. Phys. Lett. **86**, 033502 (2005); 10.1063/1.1852712

Time response characteristics of an oxide-confined GaAs AlGaAs resonant cavity-enhanced photodetector
Appl. Phys. Lett. **85**, 3011 (2004); 10.1063/1.1806267

Resonant-cavity InGaAs/InAlGaAs/InP photodetector arrays for wavelength demultiplexing applications
Appl. Phys. Lett. **70**, 2347 (1997); 10.1063/1.118870

AIP Journal of Applied Physics

Journal of Applied Physics is pleased to announce André Anders as its new Editor-in-Chief

This article is copyrighted as indicated in the article. Reuse of AIP content is subject to the terms at: http://scitation.aip.org/termsconditions. Downloaded to IP: 138.251.162.207 On: Mon, 25 Aug 2014 14:32:21

APPLIED PHYSICS LETTERS **104**, 101109 (2014)

Cavity-enhanced resonant tunneling photodetector at telecommunication wavelengths

Andreas Pfenning,[a)] Fabian Hartmann, Fabian Langer, Sven Höfling,[b)] Martin Kamp, and Lukas Worschech

Technische Physik, Physikalisches Institut, Universität Würzburg and Wilhelm Conrad Röntgen Research Center for Complex Material Systems, Am Hubland, D-97074 Würzburg, Germany

(Received 31 January 2014; accepted 27 February 2014; published online 14 March 2014)

An AlGaAs/GaAs double barrier resonant tunneling diode (RTD) with a nearby lattice-matched GaInNAs absorption layer was integrated into an optical cavity consisting of five and seven GaAs/AlAs layers to demonstrate cavity enhanced photodetection at the telecommunication wavelength 1.3 μm. The samples were grown by molecular beam epitaxy and RTD-mesas with ring-shaped contacts were fabricated. Electrical and optical properties were investigated at room temperature. The detector shows maximum photocurrent for the optical resonance at a wavelength of 1.29 μm. At resonance a high sensitivity of 3.1×10^4 A/W and a response up to several pA per photon at room temperature were found. © *2014 AIP Publishing LLC*.
[http://dx.doi.org/10.1063/1.4868429]

Because of their direct bandgap most III-V-semiconductors are particularly suitable for electro-optical applications, such as lasers, on-demand single photon sources, as well as highly sensitive light detectors.[1–6] The commonly used material system for emitters and detectors in the important telecommunication windows around 1.3 and 1.55 μm are III-V-semiconductors that are lattice-matched to InP substrates. However, this material system also has some drawbacks such as the poor performance of Bragg mirrors due to the small refractive index contrast and the small available band offsets. An alternative is the use of GaInNAs. GaInNAs can be grown pseudomorphically on GaAs, has a direct bandgap and is suitable for near infrared wavelengths applications.[7] Depending on In and N concentrations, lattice-matched growth can be achieved for a desired bandgap energy.[8] Based on this material system, lasing and light detection have been realized for the near infrared.[9–12] Recently, we presented a GaAs/AlGaAs resonant tunneling diode (RTD) with GaInNAs absorption layer for telecommunication light sensing with a sensitivity of 10^3 A/W, with the RTD serving as internal amplifier of weak electric signals, caused by photo-excited charge carriers.[13] RTDs with embedded quantum dots have even been demonstrated as single photon detectors for visible and near infrared wavelengths at cryogenic temperatures.[14–17] In the biased RTD photo-excited electron hole pairs become locally separated by the applied field, which causes a variation of the internal field and hence the transmission properties of the RTD are altered.[18–20]

Here, we report on an RTD-photosensor with a cavity-enhanced efficiency for the telecommunication wavelength range at 1.3 μm operated at room-temperature. The sensor is based on a GaAs/AlGaAs RTD with a quaternary GaInNAs absorption layer integrated in an optical cavity consisting of AlAs/GaAs distributed Bragg reflectors (DBRs). The photodetector shows a high sensitivity of 3.1×10^4 A/W and a response up to several pA per photon at room temperature.

In Fig. 1(a), a sketch of the cavity-enhanced RTD photodetector is shown together with electron microscopy images of the DBR-cavity and a ring-shaped gold contact. The cavity was designed for a resonance at the telecommunication wavelength $\lambda = 1.3$ μm and consists of an upper and a lower DBR mirror with five and seven alternating AlAs/GaAs $\lambda/4$ layers, respectively. The cavity width is 2λ, which provides enough space to embed a double barrier resonant tunneling structure (RTS), contact regions and a GaInNAs absorption layer. To guarantee optimum absorption, the GaInNAs layer is located at a field maximum, whereas the resonant tunneling structure lies within a field minimum. The samples were grown by molecular beam epitaxy on an n-type doped GaAs substrate with a doping concentration of $n = 3 \times 10^{18}$ cm^{-3}. First seven alternating n-doped GaAs/AlAs DBR mirror pairs with $n = 2 \times 10^{18}$ cm^{-3} (plus a delta doping at their interfaces) and widths $\lambda/4$ (92.9 nm for GaAs and 108.9 nm for AlAs) have been grown. Next the bottom contact region was grown. It consists of 262.5 nm n-doped GaAs with a decreasing doping concentration from $n = 1 \times 10^{18}$ to 1×10^{17} cm^{-3}. The intrinsic double barrier structure (DBS) consists of 15 nm intrinsic GaAs and two 3 nm thick $Al_{0.6}Ga_{0.4}As$ barriers embedding the 4 nm thick GaAs quantum well. On top a 5 nm thick GaAs buffer layer and 10 nm undoped $Ga_{0.89}In_{0.11}N_{0.04}As_{0.96}$ were grown. The buffer layer between the RTD double barrier and the absorption layer is essential because of defect reduction.[13] Additionally, the growth temperature was reduced from 570 °C (GaAs and AlAs) to 370 °C (for GaInNAs). The quaternary GaInNAs absorption layer has a thickness of $\lambda/2$ ($\sim$160 nm) and is n-doped with increasing doping concentration from $n = 1 \times 10^{17}$ to 1×10^{18} cm^{-3}. The GaInNAs compound semiconductor is designed for a bandgap equal the resonance of the optical cavity.[8] The top GaAs contact is 290 nm thick with $n = 1 \times 10^{18}$ cm^{-3}. The top DBR is again formed by five alternating GaAs/AlAs pairs. After the growth process, RTD mesas were fabricated by standard lithographic

a)Electronic mail: Andreas.Pfenning@physik.uni-wuerzburg.de
b)Present address: SUPA, School of Physics and Astronomy, University of St Andrews, St Andrews KY16 9SS, United Kingdom.

 © 2014 AIP Publishing LLC

This article is copyrighted as indicated in the article. Reuse of AIP content is subject to the terms at: http://scitation.aip.org/termsconditions. Downloaded to IP: 138.251.162.207 On: Mon, 25 Aug 2014 14:32:21

and dry chemical etching techniques with mesa diameters from $d = 1\,\mu m$ up to $12\,\mu m$. The bottom contact (substrate) was formed by an alloyed Ni/AuGe/Ni/Au contact. On top a Ti/Pt/Au ring shaped contact was evaporated. A polymer (benzocyclobutene (BCB)) was used for mesa isolation.

Experimental (black solid line) and simulated (green dashed line) DBR-reflection spectra are shown in Fig. 1(b) together with a simulated absorption spectrum (red dots). The reflection spectra display a resonance at $1.29\,\mu m$ and a well pronounced stop band. A quality factor of about $Q = 60$ was determined from the experimental reflection spectrum. At resonance, the absorption is 18.3% and is clearly enhanced compared to off-resonant illumination. The simulation of the reflection spectrum of the DBR-cavity was conducted by using the transfer matrix method with complex indices of refraction. An undoped structure (no absorption in the Bragg mirrors) was assumed for the calculation. A band edge absorption coefficient $\alpha = 5 \times 10^3\,cm^{-1}$ for the GaInNAs absorption layer was taken into account.[21]

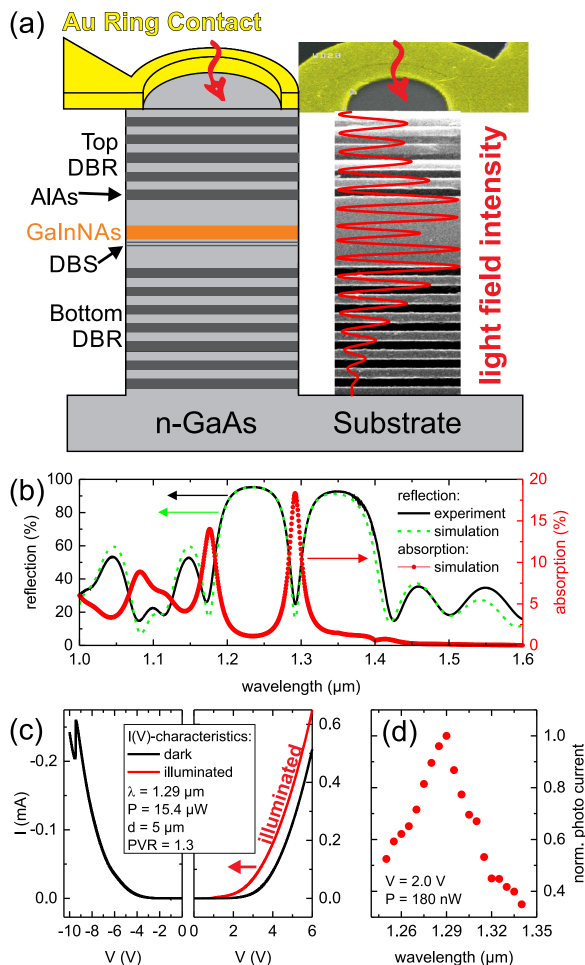

FIG. 1. The cavity enhanced RTD light detector. (a) Schematic layer structure and device layout of the cavity-enhanced RTD light detector and electron microscopy images of the DBR-cavity and an Au ring-shaped contact. The electron microscopy image includes an inset showing the distribution of the resonant light field intensity. (b) Reflection spectrum of the DBR-cavity: experimental data (black solid line) and simulation (green dashed line) with resonance at $\lambda = 1.29\,\mu m$. Simulated absorption spectrum (red dots). (c) Current-voltage characteristics at forward and reverse bias, in the dark (black solid line) and under illumination (red solid line). (d) Normalized photocurrent versus incident wavelength at a bias voltage $V = 2.0\,V$ and a constant illumination power $P = 180\,nW$. The maximum is located at the optical resonance of $1.29\,\mu m$.

Current-voltage characteristics were conducted in the dark and under illumination and are displayed in Fig. 1(c). All measurements were done at room temperature. The current was measured as voltage drop over a shunt resistance. The I(V)-characteristics exhibit a strong asymmetry caused by the asymmetric sample structure. A well pronounced negative differential conductance (NDC) region with a peak-to-valley ratio $PVR = 1.3$ is found at $V = -9\,V$ due to the transition from resonant to sequential tunneling. For positive bias the current is strongly increased, hence the RTD was operated below the NDC region in the coherent regime. When illuminated (red solid line), the positive I(V)-characteristics is shifted towards smaller voltages. Photogenerated holes from the GaInNAs layer are forced towards the RTS by the external electrical field. Here, they can accumulate and cause an additional voltage drop across the RTS, which shifts the I(V)-characteristics to smaller voltages. For negative bias no photo-effect was observed, demonstrating that no accumulation of holes nearby the RTS due to the asymmetric layout of the device takes place. The photocurrent $I_{ph} = I_{illu} - I_{dark}$ was determined by subtracting the current measured in the dark from the current detected under illumination. Fig. 1(d) shows the normalized photocurrent generated by a tunable laser for different wavelengths but constant illumination power $P = 180\,nW$. The maximum response is found at the optical resonance wavelength $\lambda = 1.29\,\mu m$.

In Fig. 2(a), the photocurrent I_{ph} of a cavity-integrated RTD with mesa diameter $d = 9\,\mu m$ is plotted versus the illumination power P at resonance wavelength ($\lambda = 1.29\,\mu m$, red circles) and 30 nm off resonance ($\lambda = 1.26\,\mu m$, blue diamonds; $\lambda = 1.32\,\mu m$, green hexagons). The working point was $V = 3\,V$. The largest response was achieved for the resonant condition due to an enhanced absorption. Since hole accumulation is a self-limiting process, I_{ph} is a nonlinear function of P, showing an asymptotic behavior. Yet, as one can see in Fig. 2(b), for weak illumination powers I_{ph} shows a linear response to P. A sensitivity $S = \Delta I_{ph}/\Delta P = 3.1 \times 10^4$ A/W was extracted. With a resonance absorption $\eta = 18.3\%$ and

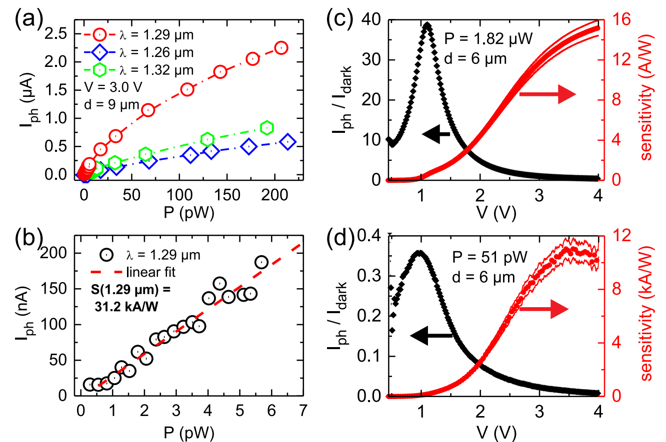

FIG. 2. Response under CW-illumination. (a) Photocurrent of an RTD with mesa diameter $d = 9\,\mu m$ versus illumination power for resonant illumination ($\lambda = 1.29\,\mu m$, red circles) and 30 nm off resonance ($\lambda = 1.26\,\mu m$, blue diamonds; $\lambda = 1.32\,\mu m$, green hexagons). (b) The sensitivity $S = 3.1 \times 10^4$ A/W in resonance is determined by the best linear fit. (c) and (d) Sensitivity S (red dots) and photocurrent to dark current ratio I_{ph}/I_{dark} of an RTD with mesa diameter $d = 6\,\mu m$ under an incident illumination power $P = 1.82\,\mu W$ (c) and 51 pW (d).

This article is copyrighted as indicated in the article. Reuse of AIP content is subject to the terms at: http://scitation.aip.org/termsconditions. Downloaded to IP: 138.251.162.207 On: Mon, 25 Aug 2014 14:32:21

the spectral response $R_\lambda = 1.04$ A/W at 1.29 μm this sensitivity corresponds to an internal gain of $M = 1.64 \times 10^5$. Compared to commercially available InGaAs/InP avalanche photodiodes which are usually operated at $M = 10$, this is an enhancement of more than four orders of magnitude.

In Figs. 2(c) and 2(d), the RTD mesa diameter here was $d = 6\,\mu$m and the sensitivity S (red dots) and the ratio of photocurrent to dark current I_{ph}/I_{dark} (black diamonds) are plotted versus bias voltage for $P = 1.82\,\mu$W (Fig. 2(c)) and $P = 51$ pW (Fig. 2(d)) with illumination at the resonance wavelength. While S gives the absolute response, I_{ph}/I_{dark} indicates the change of transmission through the RTS. The RTD sensor covers a wide power range and is most sensitive for small powers. Even though the illumination power is decreased by six decades, both figures exhibit qualitatively the same features, with a quantitative difference of three orders of magnitude. For voltages below 0.5 V the RTD is pinched off, hence S is zero. For voltages above 0.5 V, the RTD opens and photogenerated charge carriers at the RTS trigger the amplification process. S increases exponentially with V. A further increase of V leads to an enhanced hole tunneling of accumulated holes at the RTS. Thus, S decreases again. This is apparent in Fig. 2(d), where a maximum sensitivity $S \sim 1.1 \times 10^4$ A W^{-1} is reached at $V \sim 3.5$ V, whereas the maximum of I_{ph}/I_{dark} is at about $V = 1$ V.

Fig. 3 illustrates the cavity-enhanced RTD photodetector response to weak incident light pulses. In Fig. 3(a), I_{ph} is plotted versus time for pulse widths $\Delta t = 800\,\mu$s down to $2\,\mu$s. The pulses came at a repetition frequency $f = 500$ Hz. The current signal was sampled up to 10^5 times and averaged. The on-illumination power was constant at $P = 2.0$ pW, corresponding to an incident photon rate of 1.3×10^7 s^{-1}. The number of photons in a pulse is thus controlled by the pulse width. For weak light powers the photocurrent is a linear function of P, which means that the photocurrent is determined by the number N of photogenerated holes accumulated at the double barrier structure, whereas N is in turn determined by a generation rate G (illumination on/off) and an escape rate (by tunneling) $-N/\tau$, with the average hole-lifetime τ. This can be described by a simple rate equation $dI_{ph}(t) \propto dN(t) = G(t) - N(t)/\tau$. For all pulse width, I_{ph} rises exponentially, when illumination is switched on, and decreases exponentially again, when the light pulse is switched off. From the decay, hole-lifetimes can be estimated to be about $\tau \approx 100\,\mu$s. This long lifetimes indicate efficient trapping of accumulated photogenerated holes and are well comparable to hole-life-times reported for similar structures with embedded quantum dots.[14] In Fig. 3(b), I_{ph} versus time is shown for pulses of 26 (red line) and 131 (green line) photons. With $\eta = 18.3\%$ this corresponds to 5 and 24 photogenerated electron-hole pairs, respectively. Thus, the time integrated photocurrent reflects the number of photo-triggered charge carriers per pulse. Fig. 3(c) shows the photo-triggered charge versus number of incident photons per pulse. From a best linear fit an amplification factor $M = 2.31 \times 10^4$ was obtained. At $\lambda = 1.29\,\mu$m this corresponds to a sensitivity $S = 4.40 \times 10^3$ A/W, which is in good agreement with the value obtained in Fig. 2(d). An RTD with $d = 5\,\mu$m was then excited with weak resonant light pulses at a repetition frequency $f = 10.0$ kHz at $V = 2.0$ V.

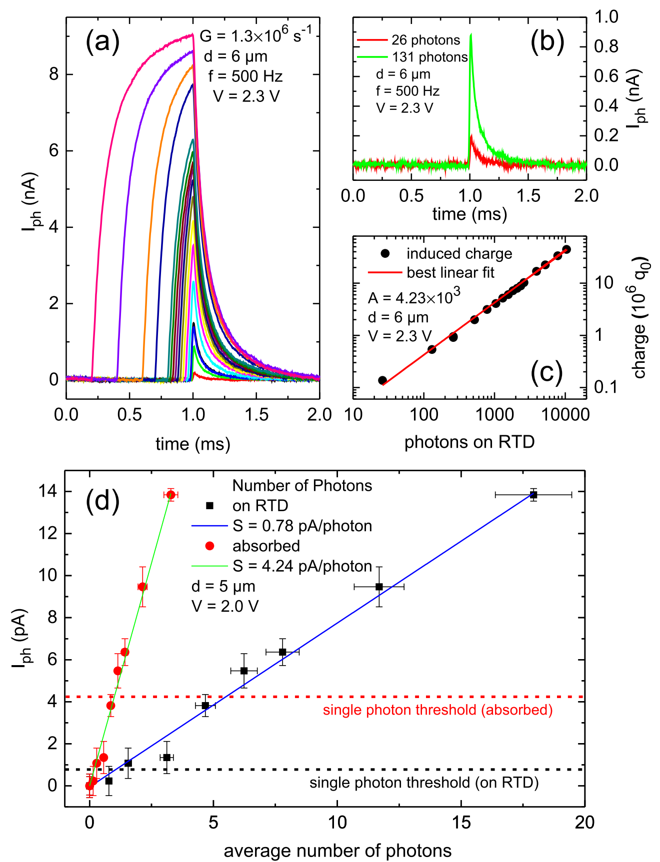

FIG. 3. Excitation with weak, resonant light pulses: (a) and (b) Photocurrent versus time of an RTD with $d = 6\,\mu$m for pulsed excitation with resonant light at $\lambda = 1.29\,\mu$m. The repetition frequency is $f = 500$ Hz, the bias voltage is $V = 2.3$ V, and the on-rate of incident photons is 1.3×10^7 s^{-1}. (c) Triggered charge versus average number of photons per pulse. (d) Photocurrent I_{ph} versus average number of photons per pulse for RTD mesa diameter $d = 5\,\mu$m, excitation frequency $f = 10.0$ kHz, $\lambda = 1.29\,\mu$m, and bias voltage $V = 2.0$ V.

The resulting photocurrent was measured with a lock-in technique and is depicted in Fig. 3(d) versus the number of incident photons (black squares) and the number of absorbed photons (red dots). A linear response of photocurrent to the number of incident photons per pulse can be seen. When the light beam is blocked (zero photons per pulse) I_{ph} is zero. For pulses which carry as average mean value less than one photon, there is still a measurable response. It was found that $I_{ph} = 0.78$ pA per incident photon, corresponding to 4.24 pA per absorbed photon.

In summary, we have fabricated and demonstrated cavity-enhanced RTD light detectors operating at room temperature. Because of their small diameter the detectors are suitable for high resolution array formation and production in large numbers. The integration into an optical DBR-cavity allows for wavelength-selective detection and enhanced quantum efficiency at a resonance wavelength of 1.29 μm. By increasing the number of DBR mirror pairs both sensitivity and wavelength-selectivity can be further enhanced. Longer wavelengths can be covered by adjusting the In and N concentration of the GaInNAs layer. Photo-excited holes accumulated in the vicinity of the RTS trigger an increased current through the double barrier structure. Sensitivities up to 3.1×10^4 A/W have been demonstrated and a response up to several pA per photon at room temperature was found.

This article is copyrighted as indicated in the article. Reuse of AIP content is subject to the terms at: http://scitation.aip.org/termsconditions. Downloaded to IP: 138.251.162.207 On: Mon, 25 Aug 2014 14:32:21

The authors are grateful for the financial support by the BMBF via national project EIPHRIK (FKZ: 13N10710), the European Union (FPVII (2007-2013) under Grant Agreement No. 318287 LANDAUER). Expert technical assistance by M. Emmerling and S. Handel is gratefully acknowledged.

[1]J. J. Coleman, Semicond. Sci. Technol. **27**, 090207 (2012).
[2]S. Buckley, K. Rivoire, and J. Vučković, Rep. Prog. Phys. **75**, 126503 (2012).
[3]R. H. Hadfield, Nat. Photonics **3**, 696 (2009).
[4]C. Schneider, T. Heindel, A. Huggenberger, T. A. Niederstrasser, S. Reitzenstein, A. Forchel, S. Höfling, and M. Kamp, Appl. Phys. Lett. **100**, 091108 (2012).
[5]Y.-M. He, Y. He, Y.-J. Wei, D. Wu, M. Atatüre, C. Schneider, S. Höfling, M. Kamp, C.-Y. Lu, and J.-W. Pan, Nat. Nanotechnol. **8**, 213 (2013).
[6]J. Claudon, J. Bleuse, N. S. Malik, M. Bazin, P. Jaffrennou, N. Gregersen, C. Sauvan, P. Lalanne, and J.-M. Gérard, Nat. Photonics **4**, 174 (2010).
[7]M. Kondow, T. Kitatani, S. Nakatsuka, M. C. Larson, K. Nakahara, Y. Yazawa, M. Okai, and K. Uomi, IEEE J. Sel. Top. Quantum Electron. **3**, 719 (1997).
[8]R. Kudrawiec, J. Appl. Phys. **101**, 023522 (2007).
[9]H. Riechert, A. Ramakrishnan, and G. Steinle, Semicond. Sci. Technol. **17**, 892 (2002).
[10]J. S. Harris, Semicond. Sci. Technol. **17**, 880 (2002).
[11]J. B. Héroux, X. Yang, and W. I. Wang, Appl. Phys. Lett. **75**, 2716 (1999).
[12]Q. Han, X. H. Yang, Z. C. Niu, H. Q. Ni, Y. Q. Xu, S. Y. Zhang, Y. Du, L. H. Peng, H. Zhao, C. Z. Tong, R. H. Wu, and Q. M. Wang, Appl. Phys. Lett. **87**, 111105 (2005).
[13]F. Hartmann, F. Langer, D. Bisping, A. Musterer, S. Höfling, M. Kamp, A. Forchel, and L. Worschech, Appl. Phys. Lett. **100**, 172113 (2012).
[14]J. Blakesley, P. See, A. Shields, B. Kardynał, P. Atkinson, I. Farrer, and D. Ritchie, Phys. Rev. Lett. **94**, 067401 (2005).
[15]S. S. Hees, B. E. Kardynal, P. See, A. J. Shields, I. Farrer, and D. A. Ritchie, Appl. Phys. Lett. **89**, 153510 (2006).
[16]H. W. Li, B. E. Kardynał, P. See, A. J. Shields, P. Simmonds, H. E. Beere, and D. A. Ritchie, Appl. Phys. Lett. **91**, 073516 (2007).
[17]H. W. Li, B. E. Kardynał, D. J. P. Ellis, A. J. Shields, I. Farrer, and D. A. Ritchie, Appl. Phys. Lett. **93**, 153503 (2008).
[18]I. J. S. Coêlho, J. F. Martins-Filho, J. M. L. Figueiredo, and C. N. Ironside, J. Appl. Phys. **95**, 8258 (2004).
[19]P. W. Park, H. Y. Chu, S. G. Han, Y. W. Choi, G. Kim, and E.-H. Lee, Appl. Phys. Lett. **67**, 1241 (1995).
[20]N. Vodjdani, F. Chevoir, D. Thomas, D. Cote, P. Bois, E. Costard, and S. Delaitre, Appl. Phys. Lett. **55**, 1528 (1989).
[21]J. Geisz, D. Friedman, J. Olson, S. R. Kurtz, and B. M. Keyes, J. Cryst. Growth **195**, 401 (1998).

This article is copyrighted as indicated in the article. Reuse of AIP content is subject to the terms at: http://scitation.aip.org/termsconditions. Downloaded to IP: 138.251.162.207 On: Mon, 25 Aug 2014 14:32:21